Bulletin of Earthquake Engineering (2020) 18:3545–3562
https://doi.org/10.1007/s10518-020-00840-0

ORIGINAL RESEARCH

Modification of the data-driven period/height relationship for buildings located in seismic-prone regions such as Quito (Ecuador)

Matthieu Perrault[1,2] · Philippe Guéguen[3] · Gastón Parra[4] · Johanna Sarango[5]

Received: 12 June 2019 / Accepted: 31 March 2020 / Published online: 9 April 2020

Abstract

The fundamental period of structures is a parameter used in structure under design and for evaluating existing structures. Data-driven methods using ambient vibrations have become popular, particularly for the adjustment of empirical relationships applied to building classes. This study presents the results of a survey of ambient vibrations performed in 146 reinforced concrete buildings in the center of Quito (Ecuador). Classical functional forms giving period (T) for height (H) or number of floors (N) are derived and compared with the relationships available in the Ecuadorian seismic design provisions. We highlight variations in the empirical relationships according to soil conditions, but above all according to the date of construction and the historic seismic sequence to which the buildings have been exposed. The cumulative damage effect is finally confirmed by repeating ambient vibration measurements after the 2016 Mw 7.8 Pedernales earthquake located in the subduction zone, about 175 km from Quito. Even with such a long epicentral distance, leading to low macroseismic intensity ($I_{EMS98} = IV$), the seismic ground motion of between 0.017 and 0.081 g recorded in Quito reduced the resonant frequency of the buildings tested by between 2 and 13%. This confirms the effect of cumulative damage in reinforced concrete buildings located in seismic zones, even for weak ground motions, and the variability of empirical T/H relationships associated with damage.

Keywords Building testing · Ambient vibration · RC buildings · Pedernales earthquake · Quito · Ecuador

Electronic supplementary material The online version of this article (https://doi.org/10.1007/s10518-020-00840-0) contains supplementary material, which is available to authorized users.

✉ Philippe Guéguen
philippe.gueguen@univ-grenoble-alpes.fr

1 Instituto Geofisico, Escuela Politécnica Nacional, Quito, Ecuador

2 MouvGS Research Team, CEREMA Méditerranée, Sophia Antipolis, France

3 ISTerre, Université Grenoble Alpes, Université Savoie Mont-Blanc, CNRS, IRD, Université Gustave Eiffel, Grenoble, France

4 Centro de Investigacion de la Vivienda, Escuela Politécnica Nacional, Quito, Ecuador

5 Escuela Poltécnica Nacional, Quito, Ecuador

1 Introduction

The seismic loadings supported by civil engineering structures are resonance frequency- (or period) and damping-dependent. The shape of the response spectrum for a given seismic demand is therefore the result of the seismic response of a series of one degree of freedom systems having a specific period of resonance for a given value of damping. Currently, the fundamental period is a parameter used in structure under design and structure retrofitting (CEN 2004). The seismic design provisions of buildings codes (e.g. Uniform Building Code in US, Eurocode in Europe) provide simplified relationships between the period (T) and the building height (H) to be used, for example, in equivalent lateral force analysis, according to the design (e.g. shear walls or frame buildings), method (force-based or displacement-based design approaches) and materials (reinforce concrete RC or steel). The empirical period formulae in the US seismic code were first established by experiments assessing structural periods from their seismic motion during Californian earthquakes (Goel and Chopra 1997, 1998). Since Carder (1936), many experiments have been conducted using ambient vibrations (AV) recorded in buildings, notably thanks to improvements in digital acquisition systems and signal processing methods for structural modal analysis. The efficiency of AV-based methods is no longer in doubt, supported by the operational modal analysis community (Brincker and Ventura 2015). Many model-driven (e.g. Crowley and Pinho 2004, 2010) or data-driven studies (e.g. Gallipoli et al. 2009; Michel et al. 2010a; Salameh et al. 2016) focus on the assessment of resonance periods of structures and the definition of T/H relationships, which are relevant to seismic risk analysis. Additional structural features, such as cracking and plan irregularity (Masi and Vona 2010) or the nature of infills (DeLuca et al. 2014), determine the empirical period formulae for concrete structures. Continuous monitoring of modal parameters has also demonstrated their high sensitivity to external forces, such as weather conditions (e.g., Clinton et al. 2006; Mikael et al. 2013; Guéguen et al. 2016), variations in soil-structure interactions (e.g., Todorovska and Al Rjoub 2006; Guéguen et al. 2017), and also a larger damping coefficient variation than the resonance frequency (e.g., Nayeri et al. 2008; Brossault et al. 2018).

Period-based operational applications for post-earthquake damage classification exploring the post/ante period ratio provide evidence of the efficiency of operational modal analysis for earthquakes. For example, using permanent instrumentation, Clinton et al. (2006), Mucciarelli et al. (2009), and Astorga et al. (2018, 2019) evaluated the variation of period values before and after damaging earthquakes, and Dunand et al. (2004) and Vidal et al. (2014) matched the period shift with operational and emergency assessment of post-earthquake damage based on visual inspection. Using AV, Dunand et al. (2004) and Vidal et al. (2014) showed that with a before/after period variation of less than 30–40%, structures remained in an undamaged grade; these values can be used as thresholds for damage occurrence for a Seismic Structural Health Monitoring (S2HM) strategy (Guéguen and Tiganescu 2018). Trevlopoulos and Guéguen (2016) provided time-variant capacity curves of RC structure models with cumulative damage, considering the resonance frequency variation as a damage proxy. Masi and Vona (2010), with modeling, and Guillier et al. (2014), with experimental data, clearly showed the high sensitivity of T/H empirical period formulae to damage and/or cracking states, especially for structures tested a long time after they were built, i.e. certainly having suffered aging or seismic damage in seismic-prone regions. However, there is still no universal relationship between the level of damage or cracking and the resonance frequency shift observed using ambient vibrations. Furthermore, it is also difficult to know to what extent the AV frequency values used to calibrate the T/H coefficients are influenced by the past seismic activity of the region and the cumulative structural damage.

The objective of this study is to examine the modal variation of existing RC structures in Quito (Ecuador) due to the 2016 Pedernales (magnitude M = 7.8) earthquake. In 2015, an experiment was conducted to obtain the resonance frequencies of buildings using ambient vibration techniques. After the earthquake, almost all the buildings were tested again to assess the potential effect of the earthquake on the structures. In the first section, we present the study area and the buildings tested. The second section describes the data acquisition and processing methods, and the results of the survey with respect to building characteristics are provided in the third section. Finally, the post-earthquake survey is presented, as well as the effect of this earthquake on the empirical relationships, and conclusions are given in the last section.

2 Dataset

The area concerned is the center part of Quito, the capital city of Ecuador (Fig. 1a), a high seismic hazard prone city (Beauval et al. 2010, 2013). Located on a hanging wall of a sedimentary valley, Quito's population counts approximately 1.6 million inhabitants in an area of approximately 370 km^2. In the last two decades, a number of seismic risk assessments have been carried out in Quito: the seismic risk management scenario project in the context of the United Nations program in the 1990s (e.g., Chatelain et al. 1999), site effect studies using seismic noise measurements (e.g., Guéguen et al. 2000),

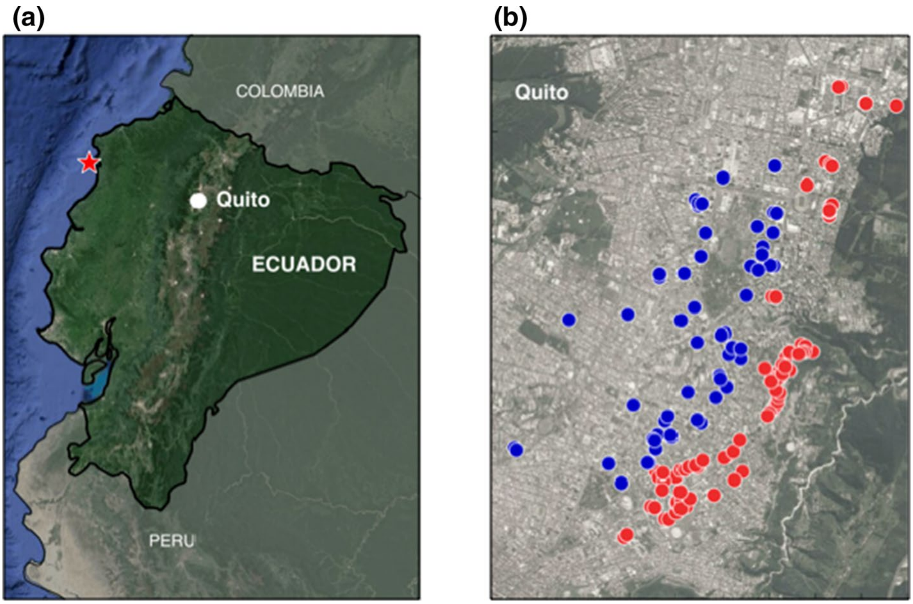

Fig. 1 Geographic location of the experiment. **a** Map of Ecuador (red star: 2016 Mw 7.8 Pedernales earthquake). **b** Location of the buildings tested in 2015 (blue: soft soil conditions; red: stiff soil conditions)

and since 2009, the installation of a permanent accelerometer network for the prediction of ground motion and site effects based on standard seismic methods (e.g., Laurendeau et al. 2017). Quito has seen substantial urban growth since the 1990s (Chatelain et al. 1999), with tall RC buildings mainly found in the urban expansion areas. Several construction codes were in use at the time of their construction, resulting in a wide variability of building design, particularly before implementation of the earthquake building code in 2002 (NEC 2002), updated in 2015 (NEC 2015).

The locations of the buildings concerned are given Fig. 1b. The color code distinguishes (1) buildings located on the soft soil (in blue) that covers the central depression of the valley, characterized by a recent lacustrine deposit causing seismic ground motion amplification (Guéguen et al. 2000), and (2) buildings on stiff soil (in red), corresponding to consolidated volcanic deposits (named Cangahua deposits), on the eastern edge of the basin. No additional information about site conditions for each building is available. A medium stiff zone is also present in the transition zone with a central depression (Chatelain et al. 1999). In this study, according to the Ecuadorian building code, the buildings concerned are non-ductile RC infilled frame structures, with more than 2 floors, i.e. the most dominant typology according to the classification by Villar-Vega et al. (2017) for the urban areas of Ecuador. In our study, 146 buildings, selected to represent as well as possible a wide range of building heights, were tested in 2015. Figure 2a represents the distribution of the buildings tested, ranging mainly between 2 and 16 floors, with some exceptionally tall buildings and a majority of 8-floor structures, i.e. the dominant typology in Quito.

Fig. 2 Distribution of the buildings tested in 2015 and 2017, according to number of floors (**a**) and year of construction (**b**). In brackets, the period considered in the manuscript with the number of buildings tested (2015/2017)

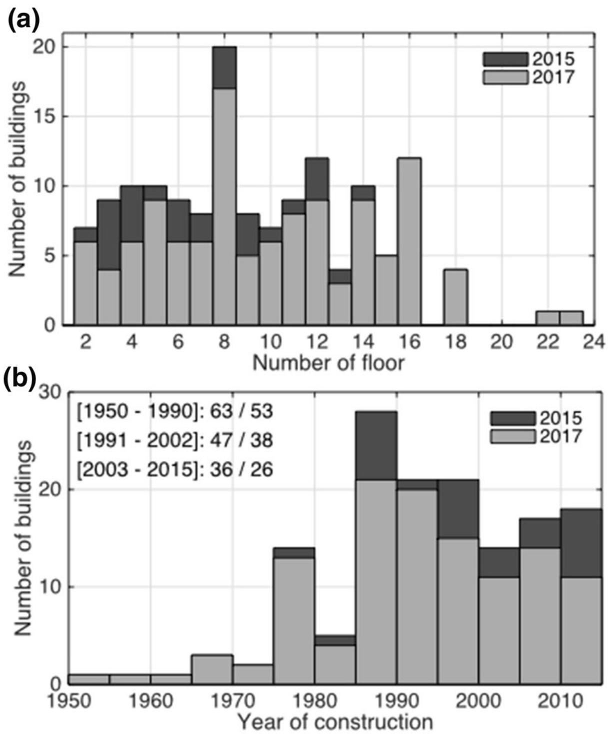

On 16 April 2016, a Mw 7.8 earthquake occurred along the Colombia-Ecuador subduction zone, typical of the historic activity (Ye et al. 2016). This earthquake caused important destruction in the epicentral region (Goretti et al. 2017), characterized by EMS98 macroseismic intensity IX (Instituto Geofisico EPN https://www.igepn.edu.ec/informes-sismicos/especiales/sism-e-2016/14805-informe-sismico-especial-n-18-2016/file last access 05/2019; Chunga et al. 2018). In Quito, located about 175 km from the epicenter, intensity was estimated at IV. Because of the small distance between buildings compared to the epicentral distance, we consider that all buildings have the same epicentral distance. According to the EMS98 intensity definition, many inhabitants felt the shaking inside their houses, some objects oscillated and no damage was expected. Despite no damage being expected, a second series of measurements was carried out on the same set of buildings, between November 2016 and March 2017, i.e. at least seven months after the main shock. The same equipment was used for the two campaigns and a similar data processing was done (see Sect. 3). Figure 2b compares the characteristics of the buildings tested in 2015 with those tested in 2016–2017. In total, only 117 buildings were tested in 2016–2017, compared with the 146 buildings tested in 2015, the difference corresponding to buildings for which the second authorization was not obtained. However, the height distribution of the buildings was the same, and the buildings covered the two geotechnical sectors presented previously.

The buildings were also selected equally according to their construction date. Guillier et al. (2014) showed a modification of structure response according to major historic earthquakes, which could have affected the real estate in Lima (Peru). In our study, three periods were defined according to the seismic activity of the region (Beauval et al. 2013), considering historic events that might have affected Quito's buildings, and according to the earthquake code applicable in 2002. Figure 3 shows the earthquake distribution according to magnitude and epicentral distance from Quito since 1950, i.e. the date of construction of the oldest building tested. Approximately 1200 events were recorded with a magnitude M > 4.5 and epicentral distance R < 500 km (USGS Catalog; https://earthquake.usgs.gov/earthquakes/browse/ last access 01/2018). The dates of the most important events are indicated. These earthquakes correspond to scientific publications or reports, and include, for example, the earthquake of Mar-1987 (Reventador, M = 7.2, R = 83 km) and the Quito quakes in Nov-1986 (5.3, 7 km) and Aug-1990 (5.3, 15 km). The 2016 Pedernales generated weak macro-seismic intensities attributed to the city. We therefore consider three different periods of construction: (1) [1950–1990] for buildings constructed before 1990, i.e.

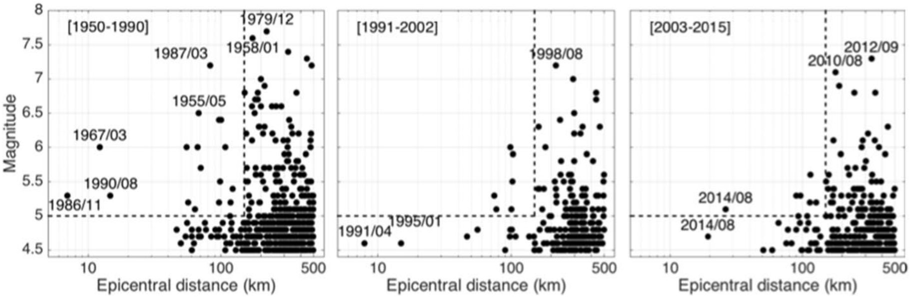

Fig. 3 Number of earthquakes according to magnitude and epicentral distance (USGS catalogue), represented for the period considered in the manuscript. Dates of the main earthquakes are indicated. Dashed lines indicate the M > 5 and R < 100 km earthquakes

the period suffering the most relevant earthquakes; (2) [1991–2002] for buildings that did not suffer relevant earthquakes and were built before the national building code changed (NEC 2002); (3) [2003–2015] for the newest buildings, designed according to the new building code. All the data (i.e., building main characteristics and resonance frequencies before and after Pedernales earthquake) are provided in electronic supplement.

3 Ambient vibration recordings

The dynamic response of the tested structures was assessed using ambient vibrations. The robustness of this approach, widely used for building testing, has been confirmed for the dynamic characterization of structures by many authors since Carder (1936), e.g. Nayeri et al. (2008), Gallipoli et al. (2009) and Michel et al. (2010a). Based on the premise that vibrations are recorded by sufficiently sensitive acquisition systems, including both digitizers and sensors, the basic process for recording and processing data consists in calculating the average Fourier spectra of ambient vibration recordings made at the top floor of the building. In this study, we chose to make three simultaneous measurements at the top with three sensors aligned in the longitudinal direction (Fig. 4); this enables physical distinction between the horizontal bending modes and the torsion mode (i.e., rotation around the vertical axis) using the Frequency Domain Decomposition method (Brincker and Ventura

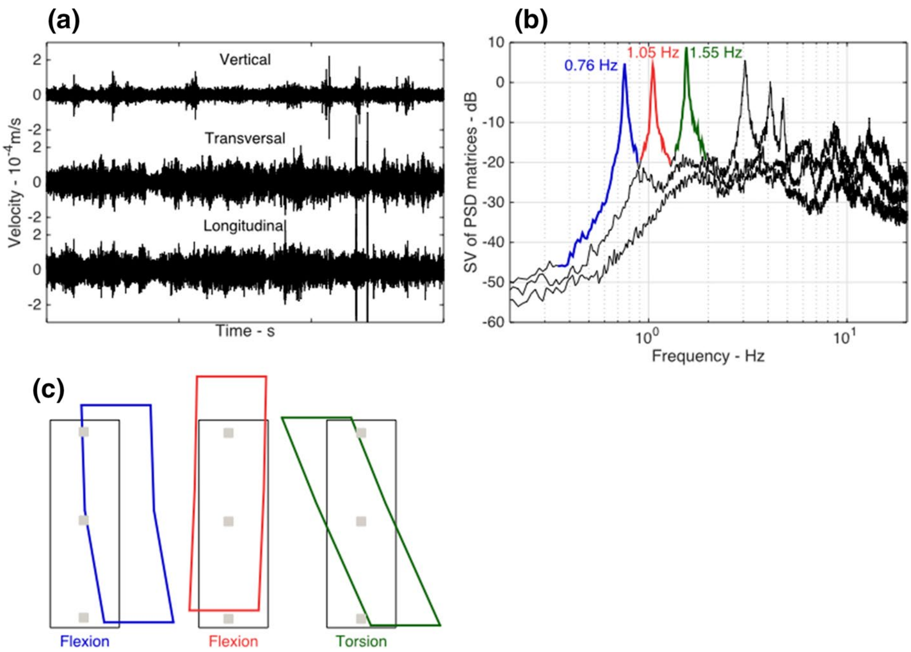

Fig. 4 Example of data processing. **a** Ambient vibrations recorded in vertical, longitudinal and transverse directions. **b** Singular values computed by Frequency Domain Decomposition. Values indicate the resonance frequencies for the horizontal modes in the transverse (blue) and longitudinal (red) directions, and torsion mode (green). Colored bandwidths of modes correspond to MAC value of 80% **c** L,T mode shapes obtained from singular value decomposition. Gray squares indicate the positions of the three 3C sensors used for modal analysis

2015). FDD is a standard operational modal analysis method validated for civil engineering structures (e.g., Michel et al. 2010b; Goulet et al. 2013; Perrault et al. 2013). It consists in computing, by singular value decomposition, the eigenvectors corresponding to the power spectral density (PSD) matrices of the recordings. This provides the eigen-modes (singular vectors, SV) and the eigen-frequencies (singular values), assuming mode orthogonality. The physical significance of the eigenvector is confirmed by applying the Modal Assurance Criterion (MAC) value, which enables discrimination between the singular value peaks of PSD matrices corresponding to physical structural modes and other SV peaks.

Figure 4 shows the process, with an example of measurements made at the top of a 16-floor building in the 2015 dataset. Synchronized data were recorded for 15 min by three sensors in the three main building directions (Fig. 4a) with Reftek stations (type REFTEK-160-03B, with a 3C geophone and an ADXL325 accelerometer). Only the geophone was used, being more sensitive, to obtain a better resolution of ambient vibrations. The data were pre-processed (mean removal, trend removal, apodization, etc.) according to the process applied by Michel et al. (2010b). SV were then calculated by FDD (Fig. 4b). The frequency bands indicated in color correspond to the 80% MAC value that confirms the physical structural modes. Eigenvectors were used to reproduce modal deformations. In our case, since only measurements at the top were available, the modal deformations are only represented in the longitudinal–transverse (L–T) plane at the roof of the structure, allowing nevertheless to distinguish the L and T bending modes from the torsion mode (Fig. 4c). In this example (Fig. 4b), 3 modes are clearly identified at $f_{1T}=0.76$ Hz, $f_{1L}=1.05$ Hz and $f_T=1.55$ Hz, for the transverse, longitudinal and torsion modes, respectively, as well as higher bending modes, over 2 Hz, in both horizontal directions. Recent studies (e.g., Boutin et al. 2005; Perrault et al. 2013; Michel and Guéguen 2018; Guéguen et al. 2019) have shown the possibility of defining the structural behavior using continuous beam like structures, whose modal characteristics generally vary between the shear ($f_i/f_1=3$, 5 [i=2,3]) and the bending ($f_i/f_1=6.3$, 17.5 [i=2,3]) beams, according to the structural design. The ratio between the second and the third modal frequencies in both horizontal directions and the fundamental mode is plotted in Fig. 5, according to building height H. From the entire dataset, only 260 and 95 data are concerned, corresponding to the number of buildings for which the second and third bending modes are assessed in the longitudinal and transverse direction. The fit to the data (Fig. 5) corresponds to the relationship:

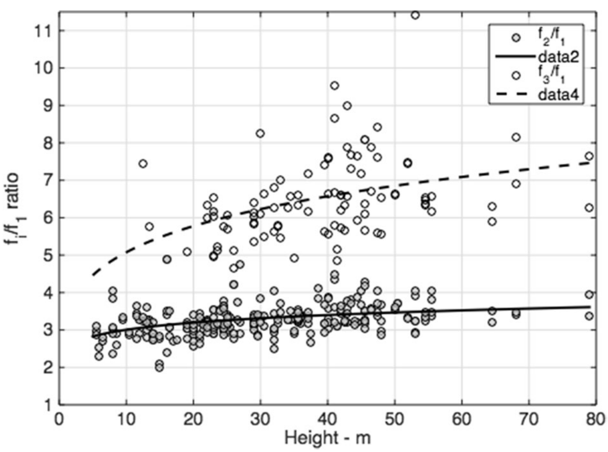

Fig. 5 Frequency ratio versus building height for the 2015 experiment, considering both horizontal components. Solid and dashed lines are the $f_x/f_1=a\cdot H^{\alpha}$ functions fitted to the data

$$f_2/f_1 = 2.450\ H^{0.089}$$

$$f_3/f_1 = 3.304\ H^{0.186}$$

Note the f_2/f_1 ratio close to 3 for the smallest buildings, i.e. corresponding to a classic shear beam model (Boutin et al. 2005; Perrault et al. 2013), typical of this type of building and increasing slightly with height (up to 3.5). The same variation is observed for the f_3/f_1 ratio: starting from 5 and increasing to 7.5, showing modification of the theoretical beam-like model with height.

In this study, period (T) or frequency (f) versus height (H, N) relationships are derived considering both horizontal directions (L and T) mixed together for each building. Actually, most of relationships found in seismic codes are provided considering the building height, without considering plan dimension. In addition Michel et al. (2010a) concluded on the low impact of the plan dimension in the dispersion of the relationships.

4 Empirical models based on period and number of floors

Figure 6 shows the relationship between the building resonance period measured in 2015 and building height, compared with the formulae from the latest national building code (NEC 2015). One of the first formulae relating the fundamental period of vibration to height, used for the simplified design of RC structures, is given in ATC3-06 (1978), as follows:

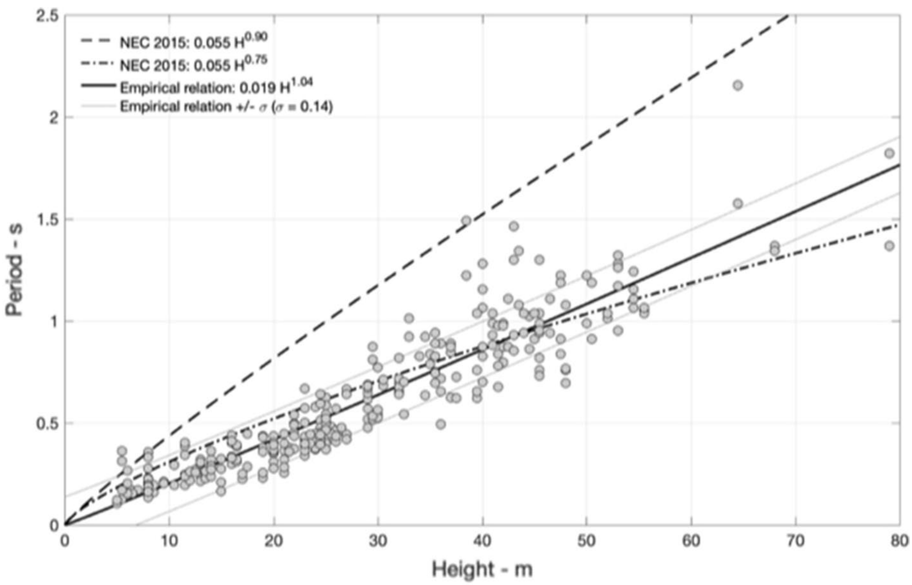

Fig. 6 Period of the first mode in the transverse and longitudinal direction (filled dot) versus the height for buildings tested in 2015, compared to the National Ecuadorian Code relationships for mixed RC structures (dashed line) and RC frame structures without structural walls or bracing elements (dashed-dotted line). Solid thick line and solid thin line correspond to the empirical model fitted to the data (± standard deviation)

$$T = CtH^{\alpha} \tag{1}$$

with C_t and α calibrated so that the fundamental period thus derived is underestimated by about 10–20%, at a yield value to obtain a conservative estimate of base shear (Goel and Chopra 1997). Earthquake provisions allow linear computation by equivalent static methods for structure design, which generally consider only the first mode, or by dynamic methods including the contribution of the higher modes. Crowley and Pinho (2010) discuss the meaning and relevance of the Ct coefficients in EC8 relationships. For equivalent static methods, they conclude on the possibility of using empirical relationships provided by seismic codes to estimate the vibration periods of constructions in design. Dynamic methods allow direct calculation of periods using the numerical method. Finally, Crowley and Pinho (2010) report differences in design base shear forces considering these two methods for structures in design, mainly because of the difference between code formulae and numerical computations involving seismic ground motion, during which structure stiffness can be reduced by up to 50%. Experimentally, civil engineering structures have shown to undergo a frequency shift of up to 30%, or about 10% of stiffness during seismic loading without damage being observed, but resulting in a co-seismic reduction of earthquake loading (Astorga et al. 2018).

Figure 6 shows code formulae for two types of design indicated in the Ecuadorian earthquake-resistant building code, i.e. RC frame structures without structural walls or bracing elements (Ct = 0.055, α = 0.90) and mixed RC structures (shear walls plus frame) with stiffening elements (Ct = 0.055, α = 0.75). The structural system of buildings investigated in Quito are frames with infilled masonry walls for low-rise buildings, and frames with concrete walls and masonry infills for medium to high rise buildings and Ct and α coefficients do not account for the contribution of the masonry to the structural elements. The experimental data fit the second period formula better, whereas we expect a better correlation with the other formula. It may result that the formula provided by the national code are not adapted to the national types of construction. However, the empirical coefficients Ct and α derived from the 2015 datasets are quite different (Ct = 0.019, α = 1.04 from experimental data and Ct = 0.055, α = 0.75 and 0.90 for the relationships provided in seismic codes, Fig. 6), which confirms the recognized advantage of data-driven methods applied to specific building typologies or even specific buildings. Differences between formulae provided by EC8 code and experimental data have been widely discussed in recent years (see Gallipoli et al. 2010 for a synthesis). Generally speaking, the differences between experimental and numerical modeling formulae are due to the non-linearity of structural response, the fractured state of the structures, soil-structure interaction, etc. Differences also exist when compared to seismic code provision formulae, raising questions about their calibration. For example, Gallipoli et al. (2010) reported that experimental data on RC buildings in different European countries were comparable but very different from the EC8 code formula. A similar observation is verified for Ecuadorian RC buildings.

Figure 7 shows the variation of the empirical formulae according to the three periods defined previously (Fig. 7a), and according to site conditions (Fig. 7b). For the sake of simplicity, these comparisons are made on a simplified relationship with T as a function of the number of floors N, as follows:

$$T = N/C \tag{2}$$

where C is the coefficient of proportionality. C equals 15.1 for all data (Fig. 7). For buildings built between 1950 and 1990, C is smaller (14.5) than for buildings built between

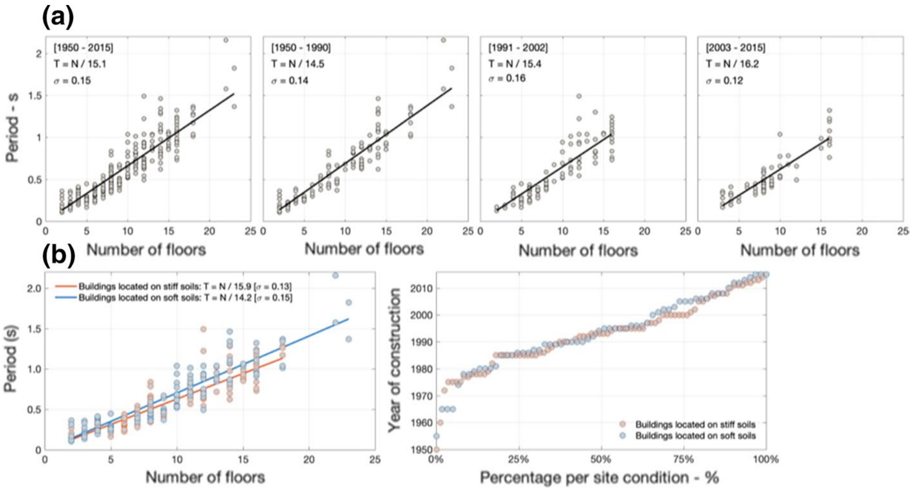

Fig. 7 Variation of the fundamental period of the buildings tested in 2015 versus the number of floors, according to construction period (**a**) and site conditions (**b**)

1991 and 2002 (C = 15.4) and between 2003 and 2015 (C = 16.2), with comparable standard variation values (between 0.12 and 0.16). For this figure and the following ones that show a regression, a linear least squares fitting is done to provide the regression and the standard deviation. During the first period, several large earthquakes were recorded (Fig. 3) which could have caused slight damage to the structures, thus reducing the frequency values (and increasing the period values). Since 1950, the buildings have undergone seismic sequences that could have affected the frequency values acquired by ambient vibrations, as already reported by Dunand et al. (2004) and Vidal et al. (2014). Using numerical simulation, Masi and Vona (2010) reported C coefficient variations of around 10% between cracked and non-cracked states of an RC structure (not caused by earthquakes). Guillier et al. (2014) also reported a variation of C values between 15 and 24 for RC buildings constructed before or after the major 1974 earthquake in Lima (Peru) and tested in 2013, corresponding to a variation of about 40%. Between [1991–2002] and [2003–2015], C values change from 15.4 to 16.2, i.e. a 5% increase. In addition, confidence interval (see Fig. 10) are different, with quite the same standard deviation. The previous and first seismic building code was released in 1977, based on the 1974 UBC, so we could expect a more important effect on the period values. Neither category suffered major earthquakes. However, Astorga et al. (2018) showed a variation of about 50% for a specific building monitored over a 20 year period in a permanently instrumented RC building. Pre-existing closed cracks can be activated even under weak loading, that can lead to a greater dispersion in the empirical relationships derived from the data collected for each typology.

Another factor influencing the empirical formulae is the boundary conditions of the structure, such as the soil-structure interaction (SSI) condition. The effect of SSI on resonance frequency has been known for a long time (e.g., Stewart et al. 1999), and is often considered or estimated for rigid structures under strong motion. Under ambient vibrations, even slight variations can be detected resulting from minor changes in soil conditions, for example due to climatic conditions (e.g., Todorovska and Al Rjoub 2006, Guéguen et al. 2017). In this study, the empirical formulae for buildings built on rock or soft soil are slightly different (Fig. 7b) with C from 15.9 to 14.2, i.e. 12% variation, with standard deviations equal to 0.13 and 0.15, respectively. As damage and SSI have the same effect on frequency (reducing resonance frequency), Fig. 7b also verifies that for each construction era, the distribution of the buildings tested on soft or stiff soil remains the same and, generally speaking, the site conditions do not have a strong impact on empirical T/N relationships computed for our dataset (Fig. 7a) over time. This effect is not negligible but remains stable over time, unlike the effect of cracking / damage.

5 Effect of the M 7.8 Pedernales (2016) earthquake on T/H models

During the April 16th, 2016 earthquake, located along the coast, many people reported strong vibrations in the structures of Quito, notably at the top of the Institute of Geophysics of the Escuela Politécnica Nacional of Quito (IG-EPN). IG-EPN building was built in 1976, prior to the first earthquake engineering regulation introduced in Ecuador. This building is a 8 stories building, each of story with the same height, each of which comprises a slab supported by reinforced concrete columns. A rough estimate of site conditions indicates a positioning of the building on very compacted volcanic deposits, similar to rock site conditions (Vs > 800 m/s). Since 2011, the structure has been permanently monitored with a triaxial accelerometer (GURALP-5TD) located at the top. Peak ground acceleration recorded in the city of Quito by the Ecuadorian network was between 0.017 and 0.081 g (Beauval et al. 2017) and macroseismic intensity evaluated at IV, i.e. no important damage was expected in Quito.

A permanent accelerometric station was installed at the top of the IG-EPN building before the 2016 earthquake. Figure 8 shows the time variation of the resonance frequency of the building, calculated on the continuous data using the Random Decrement method (Cole 1968). The data are processed to have a frequency value per day according to the procedures applied in Mikael et al. (2013) and Guéguen et al. (2017). Before the main shock, the resonance frequency of the building under ambient vibrations in both directions was between 1.5 and 1.6 Hz. During the event, a large co-seismic drop was observed, and the frequency value fell approximately to 1.1 Hz in the longitudinal direction and 1.3 Hz in the transverse direction, i.e. a variation of about 30%. Because we get only a value per day, the frequencies are smoothed and a higher coseismic drop is even expected.

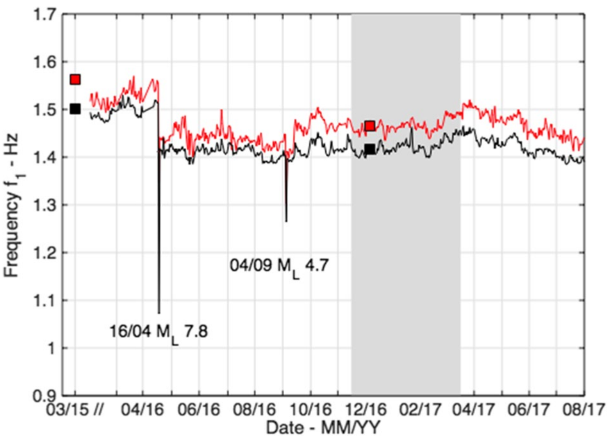

Fig. 8 Continuous monitoring of the EPN-IG building during the seismic sequence of the M7.8 Pedernales earthquake. Red and black lines correspond to the resonance frequencies in the longitudinal and transverse directions respectively. Black squares represent the date of measurement of the fundamental period. The gray zone corresponds to the period of the experimental survey performed after the Pedernales earthquake in 117 buildings

Such variations are not exceptional and are often observed under severe stress (Clinton et al. 2006; Astorga et al. 2018). After the earthquake, the resonance frequency in both directions recovered partially, with values of around 1.4 Hz, i.e. a loss of frequency of approximately 5–10% after the earthquake. Figure 8 also shows the time of the ambient vibration campaigns carried out in this study. Depending on the time of the measurement, slight fluctuations in values occur, mainly because of atmospheric conditions. Such fluctuations have been estimated for a large number of buildings and are between 1 and 2% in general (e.g., Clinton et al. 2006; Todorovska and Al Rjoub 2006; Nayeri et al. 2008; Mikael et al. 2013; Guéguen et al. 2016), i.e. less than the variations observed before/after damaging earthquakes. In Dunand et al. (2004) and Vidal et al. (2014), the frequency dropped by between 5 and 30% for buildings classified in the first level of damage. After the main shock, the fluctuation may also be due to the long recovery time of elastic properties, reflecting a slow dynamic process described by Guéguen et al. (2016) and Astorga et al. (2018) in civil engineering structures, and characteristic of the level of fracturing (Astorga et al. 2019). However, in the shaded band in Fig. 8, which corresponds to the post-seismic period of the 2016–2017 dataset, eight to eleven months after the Mw 7.8 earthquake, the frequency drop is permanent, of greater amplitude than the natural fluctuation of the resonance frequency in the particular case of the IG-EPN building, an observation that can be generalized to most of the RC buildings tested in Quito. For this particular building, the only one permanently instrumented in the city, a long-term frequency drop was only observed after the Pedernales earthquake and the aftershocks sequence. We assume the other buildings had a similar behavior, i.e. the changes observed for the second campaign were caused by the main shock and the aftershocks sequence. Furthermore, compared with the pre-event period (Fig. 5), using the same building set and the same fitting model, the ratio between the first and the second or third modes has changed slightly (Fig. 9). The fit to the data (Fig. 9) corresponds to:

$$f_2/f_1 = 2.171\ H^{0.123}$$

$$f_3/f_1 = 2.672\ H^{0.245}$$

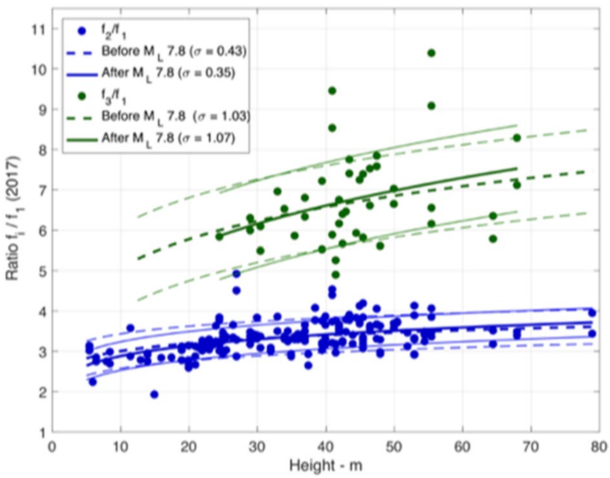

Fig. 9 Frequency ratio (blue: f_2/f_1—green: f_3/f_1) versus building height for the 2017 experimental survey. Solid and dashed lines are the $f_x/f_1 = a.H^{\alpha}$ function fitted to the data in 2017 and in 2015 given in Fig. 5. Thick and thin lines are mean ± standard deviation, respectively

The post-earthquake variation corresponds to a reduction of 10–20% for the slope of the fit and an increase of 30–40% for the exponent for both f_2/f_1 and f_3/f_1 ratios. According to the theoretical beam-like model (Perrault et al. 2013), which provides suite of frequency ratio in relation to the building design (shear to bending beam model), even if we observe changes (slight) of the frequencies, we observe no consistent change in frequencies ratios, so that the global behavior of the buildings remains the same. The variation is very slight and may have no consequence on seismic response, but it may indicate a link between damage and modification of the behavior of existing structures in the case of extensive damage.

Figure 10 shows the variation of the empirical formulae before and after the 2016 earthquake according to the number of floor (a) and the height (b). Only 117 of the 146 buildings tested in 2015 were tested in 2017. A slight variation of the empirical relationship is observed. In 2015, the values of C are identical for the whole dataset (146 buildings) and for only the 117 buildings of the 2017 dataset. Coefficient C falls from 15.14 to 14.35 between the 2015 and 2016–2017 datasets, i.e. a decrease of 5%, with a standard deviation that remains the same (0.15 before and 0.16 after). This reflects the fact that there is no physical meaning to expect a reduction of the variability after the Pedernales earthquake that did not produce strong damage. Because of the stable value of standard deviation, the difference of the mean trend, even slight, suggests a global modification of the vibration period within the dataset.

Figure 11a, b show the changes of the fundamental period according to the horizontal direction considered, compared with the height of the buildings. We observe that the frequency ratio is depending on the building height. A different trend is observed for the two directions, the ratio decreasing for taller buildings in their longitudinal direction, whereas it remains constant (around 0.956) in their transverse direction, as a consequence of the different building design in these two directions. This difference cannot fully be explained because all the buildings have a different azimuth, which means all the longitudinal directions of the buildings can be orientated in any direction.

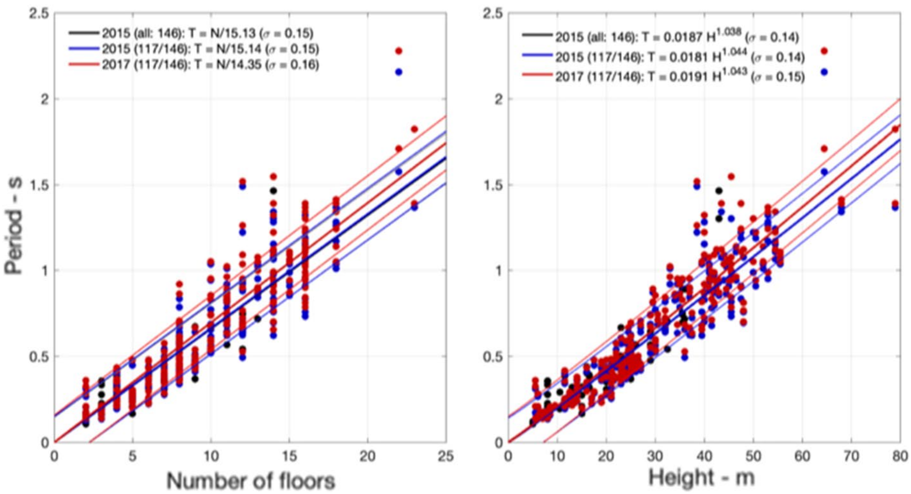

Fig. 10 Comparison of the empirical models derived from the experimental survey done before (black for all buildings; blue: for 117/148 buildings) and after (red) 2017 with number of stories or height of the building. Dots correspond to the data. Thick and thin lines are mean value of the regression ± standard deviation, respectively

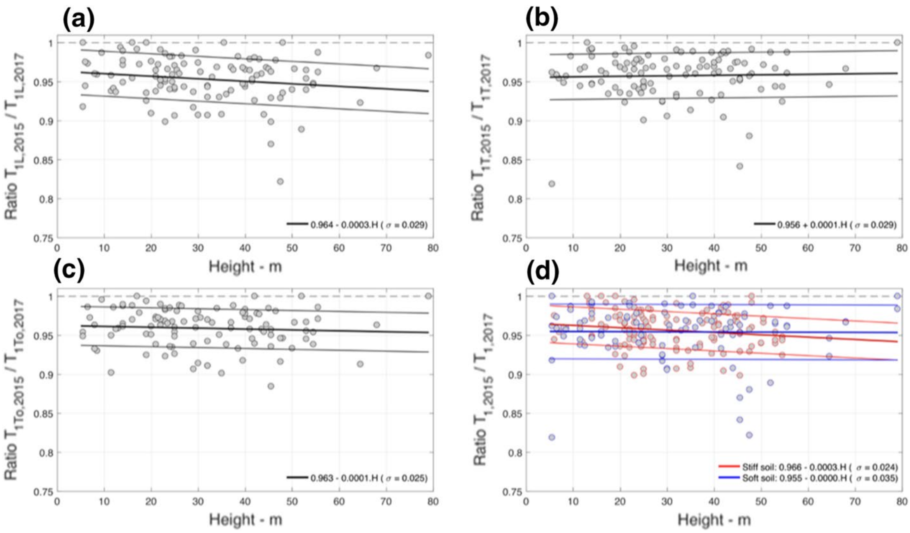

Fig. 11 Period elongation of the tested buildings between before and after the Pedernales earthquake. **a** For the first horizontal mode in the longitudinal direction (T_{1L}). **b** For the first horizontal mode in the transverse direction (T_{1T}). **c** For the first torsional period measured before and after the earthquake (T_{1To}). **d** For the first horizontal mode in both horizontal direction considering the type of soil (stiff or soft). Thick and thin lines are mean value of the regression ± standard deviation, respectively. The hashed horizontal line is the frequency value at 1

The period ratio before/after for the first torsional mode (Fig. 11c) shows a similar trend than the one observed for the horizontal direction, i.e. a higher change is observed for the tallest buildings. For the periods of both horizontal directions, and for the torsional mode, a similar standard deviation (0.029 and 0.025) is associated to the data.

Finally, Fig. 11d show the before/after period ratio of the first horizontal mode, for both directions, considering site conditions. We observe a change of period related to the height for only buildings located on stiff soil. Nevertheless a 45% higher standard deviation is associated to the soft soil data (0.035 and 0.024 for soft and rock soil data, respectively). Since the period recorded using ambient vibration corresponds to the period of the soil-structure system, this largest variability may result of the larger variability of the soft site conditions than of the rock site condition.

Even if the measurements for the 2015 and 2016–2017 datasets were not performed under the same atmospheric conditions, the frequency shift is larger than the variation expected from atmospheric conditions. Even for slight seismic ground motion, structure degradation occurs. Although it remains negligible with respect to the safety of the building stock, it is not negligible over the lifetime of a building if a long sequence of earthquakes is considered, as indicated by the variations of C in Fig. 7a or the results of Guillier et al. (2014). In practice, three categories of frequency variation are defined: [2–5%], [5–10%] and [10–13%]. Figure 12 shows the distribution of the frequency variation in Quito, according to these three categories. All the buildings tested showed a frequency variation, even though Quito city was classified as intensity IV. These variations remain larger than the seasonal variations that might be expected. No general trend is observed and no particular spatial pattern can be distinguished on the distribution of frequency variations or the number of floors.

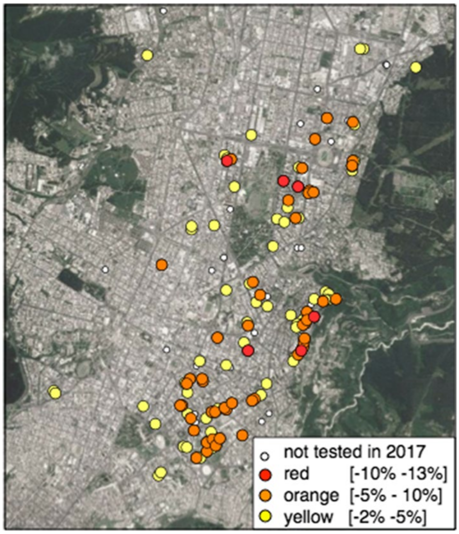

Fig. 12 Geographic location of the buildings tested in 2017, classified according to the frequency shift compared with 2015 values

However, a single earthquake may cause frequency variations impacting the change in the T/H empirical relationship T = N/C or $T = C_t\ H$. For a large number of buildings in the same typology class and located in seismic prone regions, the uncertainty of the frequency values for buildings whose period of construction covers several decades is essentially caused by the cumulative damage of successive earthquakes. This observation also reflects the high sensitivity of the dynamic parameters of structures to seismic loading and confirms the need for studies based on specific building measurements rather the empirical formulae from seismic provisions.

6 Conclusions

This study shows the effect of cumulative damage on the resonant period of RC buildings and the impact on empirical formulae derived from experimental measurements. The effect of seismic ground motion on periods has been known for a long time, especially during strong earthquakes. The level of damage can be characterized in proportion to a frequency drop (Dunand et al. 2004; Vidal et al. 2014) and, over the lifetime of structures, the accumulation of damage leads to a long-term cumulative increase in period values (Clinton et al. 2006; Astorga et al. 2018, 2019), which modifies the seismic vulnerability of existing structures. During a main shock/aftershock sequence, this period can be used as a parameter to characterize the temporal variation of seismic vulnerability over a short time, contributing to immediate post-seismic crisis management (Trevlopoulos and Guéguen 2016).

In this study, past earthquakes that shook existing buildings introduce variability in the proportionality coefficients between T and H when fitting the empirical T as a function of H relationships to the experimental data. No major damage was reported in the building tested and the slight variation of the frequency values can be interpreted as a slow degradation (similar to aging) of the building due to repeating earthquake loadings. However, this variation is slight, but not negligible, representing 5–10% depending on the RC structures tested, which may have an impact on seismic loading. In Quito, the coefficients of the relationship $T = C_t\ H$ are

Ct = 0.02 and alpha = 1.03 for all buildings, corresponding to a simplified relationship according to the number of floors N, equal to T = N/15.1 (sigma = 0.15). Depending on construction era and history, these formulae change between N/14.5, N/15.4 and N/16.2 from older to newer buildings based on the 2015 survey only. One reason invoked may be the effect of cumulative seismic damage on vibration periods, including additional effects such as aging, fatigue etc. …In this study, we have chosen to present most of the results by a simplified T = N/C relationship, in order to test the sensitivity of this relationship. Only regular buildings, geometrically in plan and elevation, were chosen in order to limit the bias due to anomalies. Fluctuations may result from internal variations in the dimensions of each floor, but this information is not easily obtained in practice. The relationships from the seismic codes provide the first approximation of the fundamental periods for some standardized constructions. Individual studies of buildings may make a relevant contribution to the reduction of building response uncertainties compared to averaged code provisions.

Quito is a high seismic hazard prone city and during the construction periods of the tested buildings, there were a number of earthquakes considered strong in terms of earthquake engineering. The occurrence of past earthquakes results in the cumulative degradation of buildings over time. Moreover, following the 2016 Pedernales earthquake, post-seismic measurements show a period increase for all the buildings tested, even though seismic ground motion was weak. The post-earthquake empirical formula gives T = N/14.3, compared with N/15.1 before the earthquake, which shows that a complete sequence of moderate to strong earthquakes makes a relevant contribution to the variability of experimental formulae. Even if Pedernales earthquake is not relevant for seismic engineering (Fig. 3), the general period elongation confirms that the tested buildings have suffered slight damage. That can then be confirmed (also with Fig. 7a) that older buildings must have been affected by a long sequence of earthquakes, even considered of low relevance to seismic engineering. Although ambient vibration measurements are currently the most efficient (cheap, fast, accurate, easily reproducible) way of evaluating the dynamic characteristics of a structure, accounting for its current condition, specific studies on the threshold level of the seismic ground motion that causes cracking or damage would help to clarify the uncertainty of T–H formulae. The fundamental period of existing buildings can change after a large but distant and seemingly undamaged earthquake, that may question on the variability of previous empirical relationships and the modification of the building properties over time. Additional information such as age, regularity of the floor plan, details of construction, foundation soil and higher modes could be integrated in further studies but for a dataset with a more detailed information.

Acknowledgements This work was supported by the French Project REMAKE (Seismic Risk in Ecuador: Mitigation, Anticipation, and Knowledge of Earthquakes, ANR-15-CE04-0004), by the Ecuadorian Project SENPLADES (Generación de capacidades para la difusión de alertas tempranas y para el desarrollo de instrumentos de decisión ante las amenazas sísmicas y volcánicas dirigidos al Sistema nacional de gestión de riesgos), and by a Grant from Labex OSUG@2020 (Investissements d'avenir, ANR10-LABX56). The authors would like to thank Juan Gabriel Barros, and Christian Viracucha for their help with the experimental surveys. We would like to especially thank Juan Carlos Singaucho (IG-EPN) for sharing his knowledge of Ecuadorian regulations and the design of the buildings in Quito.

References

Astorga A, Guéguen P, Kashima T (2018) Nonlinear elasticity observed in buildings during a long sequence of earthquakes. Bull Seismol Soc Am 108(3A):1185–1198

Astorga A, Guéguen P, Rivière J, Kashima T, Johnson PA (2019) Recovery of the resonance frequency of buildings following strong seismic deformation as a proxy for structural health. Struct Health Monit. https://doi.org/10.1177/1475921718820770

ATC3-06 (1978) Tentative provisions for the development of seismic regulations for buildings. Report No. ATC3-06. Applied Technological Council. Palo Alto, Calif

Beauval C, Yepes H, Bakun WH, Egred J, Alvarado A, Singaucho JC (2010) Locations and magnitudes of historical earthquakes in the Sierra of Ecuador (1587–1996). Geophys J Int 181(3):1613–1633

Beauval C, Yepes H, Palacios P, Segovia M, Alvarado A, Font Y et al (2013) An earthquake catalog for seismic hazard assessment in Ecuador. Bull Seismol Soc Am 103(2A):773–786

Beauval C, Marinière J, Laurendeau A, Singaucho JC, Viracucha C, Vallée M et al (2017) Comparison of observed ground-motion attenuation for the 16 April 2016 Mw 7.8 Ecuador megathrust earthquake and its two largest aftershocks with existing ground-motion prediction equations. Seismol Res Lett 88(2A):287–299

Boutin C, Hans S, Ibraim E, Roussillon P (2005) In situ experiments and seismic analysis of existing buildings Part II: seismic integrity threshold. Earthq Eng Struct Dyn 34(12):1531–1546

Brincker R, Ventura C (2015) Introduction to operational modal analysis. Wiley, Hoboken

Brossault MA, Roux P, Guéguen P (2018) The fluctuation–dissipation theorem used as a proxy for damping variations in real engineering structures. Eng Struct 167:65–73

Carder DS (1936) Observed vibrations of buildings. Bull Seismol Soc Am 26(3):245–277

CEN (2004) Eurocode 8: design of structures for earthquake resistance, Part 1: General rules, seismic actions and rules for buildings, Comite Européen de Normalisation, Brussels, Ref No. 1998-1:2004:E.

Chatelain JL, Tucker B, Guillier B, Kaneko F, Yepes H, Fernandez J et al (1999) Earthquake risk management pilot project in Quito. Ecuador GeoJ 49(2):185–196

Chunga K, Livio F, Mulas M, Ochoa-Cornejo F, Besenzon D, Ferrario MF, Michetti AM (2018) Earthquake Ground Effects and Intensity of the 16 April 2016 M w 7.8 Pedernales, Ecuador, Earthquake: implications for the source characterization of large subduction earthquakes. Bull Seismol Soc Am 108(6):3384–3397

Clinton JF, Bradford SC, Heaton TH, Favela J (2006) The observed wander of the natural frequencies in a structure. Bull Seismol Soc Am 96(1):237–257

Cole HA (1968) On-the-line analysis of random vibrations. AIAA Paper 1968; No. 68-288.

Crowley H, Pinho R (2004) Period-height relationship for existing European reinforced concrete buildings. J Earthq Eng 8(spec01):93–119

Crowley H, Pinho R (2010) Revisiting Eurocode 8 formulae for periods of vibration and their employment in linear seismic analysis. Earthq Eng Struct Dyn 39(2):223–235

De Luca F, Verderame GM, Gómez-Martínez F, Pérez-García A (2014) The structural role played by masonry infills on RC building performances after the 2011 Lorca, Spain, earthquake. Bull Earthq Eng 12(5):1999–2026

Dunand F, Ait Meziane Y, Guéguen P, Chatelain JL, Guillier B, Ben Salem R et al (2004) Utilisation du bruit de fond pour l'analyse des dommages des bâtiments de Boumerdes suite au séisme du 21 mai 2003. Mémoires du Service Géologique de l'Algérie 12:177–191

Gallipoli MR, Mucciarelli M, Vona M (2009) Empirical estimate of fundamental frequencies and damping for Italian buildings. Earthq Eng Struct Dyn 38(8):973–988

Gallipoli MR, Mucciarelli M, Šket-Motnikar B, Zupanćić P, Gosar A, Prevolnik S et al (2010) Empirical estimates of dynamic parameters on a large set of European buildings. Bull Earthq Eng 8(3):593–607

Guéguen P, Chatelain JL, Guillier B, Yepes H (2000) An indication of the soil topmost layer response in Quito (Ecuador) using noise H/V spectral ratio. Soil Dyn Earthq Eng 19(2):127–133

Guéguen P, Johnson P, Roux P (2016) Nonlinear dynamics induced in a structure by seismic and environmental loading. J Acoust Soc Am 140(1):582–590

Guéguen P, Langlais M, Garambois S, Voisin C, Douste-Bacqué I (2017) How sensitive are site effects and building response to extreme cold temperature? The case of the Grenoble's (France) City Hall building. Bull Earthq Eng 15(3):889–906

Guéguen P, Tiganescu A (2018) Consideration of the effects of air temperature on structural health monitoring through traffic light-based decision-making tools. Shock Vib. https://doi.org/10.1155/2018/9258675

Guéguen P, Mercerat ED, Alarcon F (2019) Parametric study on the interpretation of wave velocity obtained by seismic interferometry in beam-like buildings. Bull Seismol Soc Am 109(5):1829–1842. https://doi.org/10.1785/0120190054

Guillier B, Chatelain JL, Tavera H, Perfettini H, Ochoa A, Herrera B (2014) Establishing empirical period formula for RC buildings in Lima, Peru: evidence for the Impact of Both the 1974 Lima earthquake and the application of the Peruvian seismic code on high-rise buildings. Seismol Res Lett 85(6):1308–1315

Goel RK, Chopra AK (1997) Period formulas for moment-resisting frame buildings. J Struct Eng 123(11):1454–1461

Goel RK, Chopra AK (1998) Period formulas for concrete shear wall buildings. J Struct Eng 124(4):426–433

Goretti A, Hutt CM, Hedelund L (2017) Post-earthquake safety evaluation of buildings in Portoviejo, Manabí province, following the Mw7.8 Ecuador earthquake of April 16, 2016. Int J Disaster Risk Reduct 24:271–283

Goulet JA, Michel C, Smith IF (2013) Hybrid probabilities and error-domain structural identification using ambient vibration monitoring. Mech Syst Signal Process 37(1–2):199–212

Laurendeau A, Courboulex F, Bonilla LF, Alvarado A, Naya VA, Guéguen P et al (2017) Low-frequency seismic amplification in the Quito Basin (Ecuador) revealed by Accelerometric recordings of the RENAC network. Bull Seismol Soc Am 107(6):2917–2926

Masi A, Vona M (2010) Experimental and numerical evaluation of the fundamental period of undamaged and damaged RC framed buildings. Bull Earthq Eng 8(3):643–656

Michel C, Guéguen P (2018) Interpretation of the velocity measured in buildings by seismic interferometry based on Timoshenko beam theory under weak and moderate motion. Soil Dyn Earthq Eng 104:131–142. https://doi.org/10.1016/j.soildyn.2017.09.031

Michel C, Guéguen P, Lestuzzi P, Bard PY (2010a) Comparison between seismic vulnerability models and experimental dynamic properties of existing buildings in France. Bull Earthq Eng 8(6):1295–1307

Michel C, Guéguen P, El Arem S, Mazars J, Kotronis P (2010b) Full-scale dynamic response of an RC building under weak seismic motions using earthquake recordings, ambient vibrations and modelling. Earthq Eng Struct Dyn 39(4):419–441

Mikael A, Gueguen P, Bard PY, Roux P, Langlais M (2013) The analysis of long-term frequency and damping wandering in buildings using the random decrement technique. Bull Seismol Soc Am 103(1):236–246

Mucciarelli M, Bianca M, Ditommaso R, Gallipoli MR, Masi A, Milkereit C et al (2009) (2011) Far field damage on RC buildings: the case study of Navelli during the L'Aquila (Italy) seismic sequence. Bull Earthq Eng 9(1):263–283

Nayeri RD, Masri SF, Ghanem RG, Nigbor RL (2008) A novel approach for the structural identification and monitoring of a full-scale 17-story building based on ambient vibration measurements. Smart Mater Struct 17(2):025006

NEC (2002) Norma Ecuatoriana de la Construcción—NEC 2002. Código: Peligro Sísmico -Diseño Sismo Resistente; Código: NEC-SE-DS

NEC (2015) Norma Ecuatoriana de la Construcción—NEC 2015. Código: Peligro Sísmico -Diseño Sismo Resistente; Código: NEC-SE-DS

Perrault M, Gueguen P, Aldea A, Demetriu S (2013) Using experimental data to reduce the single-building sigma of fragility curves: case study of the BRD tower in Bucharest. Romania Earthq Eng Eng Vib 12(4):643–658

Salameh C, Guillier B, Harb J, Cornou C, Bard PY, Voisin C, Mariscal A (2016) Seismic response of Beirut (Lebanon) buildings: instrumental results from ambient vibrations. Bull Earthq Eng 14(10):2705–2730

Stewart JP, Seed RB, Fenves GL (1999) Seismic soil-structure interaction in buildings. II: empirical findings. J Geotech Geoenviron Eng 125(1):38–48

Todorovska MI, Al Rjoub Y (2006) Effects of rainfall on soil–structure system frequency: examples based on poroelasticity and a comparison with full-scale measurements. Soil Dyn Earthq Eng 26(6–7):708–717

Trevlopoulos K, Guéguen P (2016) Period elongation-based framework for operative assessment of the variation of seismic vulnerability of reinforced concrete buildings during aftershock sequences. Soil Dyn Earthq Eng 84:224–237

Vidal F, Navarro M, Aranda C, Enomoto T (2014) Changes in dynamic characteristics of Lorca RC buildings from pre-and post-earthquake ambient vibration data. Bull Earthq Eng 12(5):2095–2110

Villar-Vega M, Silva V, Crowley H, Yepes C, Tarque N, Acevedo AB et al (2017) Development of a fragility model for the residential building stock in South America. Earthq Spectra 33(2):581–604

Ye L, Kanamori H, Avouac JP, Li L, Cheung KF, Lay T (2016) The 16 April 2016, Mw 7.8 (Ms 7.5) Ecuador earthquake: a quasi-repeat of the 1942 Ms 7.5 earthquake and partial re-rupture of the 1906 Ms 8.6 Colombia-Ecuador earthquake. Earth Planet Sci Lett 454:248–258